FISEVIER

Contents lists available at ScienceDirect

Materials Science & Engineering A

journal homepage: www.elsevier.com/locate/msea



Structure and hardness of B2 ordered refractory AlNbTiVZr $_{0.5}$ high entropy alloy after high-pressure torsion



N.D. Stepanov^{a,*}, N.Yu. Yurchenko^a, A.O. Gridneva^a, S.V. Zherebtsov^a, Yu.V. Ivanisenko^b, G.A. Salishchev^a

ARTICLE INFO

Keywords: High entropy alloys High-pressure torsion B2 phase Laves phase Disordering Young's modulus

ABSTRACT

High-pressure torsion (HPT) at room temperature was applied to an AlNbTiVZr $_{0.5}$ refractory high entropy alloy. In the initial as-cast condition the alloy was composed of a coarse-grained B2 matrix phase and a continuous network of C14 Laves phase particles with the volume fraction of 19%. HPT resulted in the formation of a nanocrystalline structure in the B2 matrix with an average size of grains/subgrains of 25 nm after 5 revolutions. The B2 phase also underwent significant disordering during HPT. The Laves phase network was broken and individual particles became much thinner in comparison with those in the initial condition. Microhardness measurements have revealed typical of HPT gradient along the radius which decreased with increasing the number of revolutions. It was also found that the nanohardness of the B2 phase increased after HPT while the nanohardness of the Laves phase decreased. A strong decrease in the Young's modulus of the B2 phase was also found. Factors governing structure and properties evolution of the alloy during HPT were discussed.

1. Introduction

The so-called high entropy alloys (HEAs) attract a lot of attention from the researchers worldwide in recent years [1-4]. According to the original definition, HEAs are the alloys which composed of at least 5 elements in approximately equiatomic proportions [5]. The HEA concept provides enormous capabilities for novel alloys development for advanced applications [4,6]. Many produced HEAs have been considered as promising structural materials due to high strength, ductility, fracture and impact toughness [1,7-12]. One of the particularly attractive features of some HEAs is their high strength at elevated temperatures. For instance, HEAs composed of refractory elements (usually referred to as refractory HEAs) can have the superior specific strength to widely-used Ni-based super-alloys at temperatures up to 1000-1200 °C [13-20].

In most studies, HEAs are examined either in the as-cast condition or after heat treatment. Thermomechanical processing which can eliminate casting defects or refine the microstructure is generally used for highly ductile HEAs, which can be easily processed at room temperature [21–23]. The refractory HEAs usually possess limited ductility at low temperatures [13–20]. The only known exception is the HfNbTaTiZr alloy that can be cold-rolled to high thickness reductions at room temperature [24–27].

Processing of alloys with poor workability at low temperatures can be performed using special metal-working techniques. One of these techniques is high-pressure torsion (HPT) which is attractive due to the following capabilities: (i) processing of even brittle materials at room temperature; (ii) imposing almost unlimited strain; (iii) formation of an ultra-fine grained or even nanocrystalline structure as a result of such severe straining [28]. The application of HPT to various HEAs was already reported in some recent manuscripts [23,29–32]; however, highly-ductile alloys were used in the most studies. Processing of refractory HEAs by HPT is almost unexplored [33,34].

In the present work, we report structure and hardness of the refractory AlNbTiVZr $_{0.5}$ alloy after HPT processing. The alloy has demonstrated attractive mechanical properties both at room and elevated temperatures [35,36]. The structure of the alloy is composed of the (i) B2 ordered matrix phase and (ii) second Laves phase particles [36]. The effect of HPT on ordered structures or second phases evolution in HEAs has never been reported so far.

2. Materials and methods

The alloy with a nominal composition of $AlNbTiVZr_{0.5}$ (the subscript indicates the molar fractions of the corresponding element; if the molar fraction is unity the subscript is omitted) was produced by arc

^a Laboratory of Bulk Nanostructured Materials, Belgorod State University, Belgorod 308015, Russia

^b Karlsruhe Institute of Technology, Institute of Nanotechnology, Karlsruhe, Germany

^{*} Correspondence to: Laboratory of Bulk Nanostructured Materials, Belgorod State University, Pobeda 85, Belgorod 308015, Russia. E-mail addresses: stepanov@bsu.edu.ru, stepanov.nikita@icloud.com (N.D. Stepanov).

Table 1 The chemical composition of the structural constituents of the AlNbTiVZ $r_{0.5}$ alloy in the initial (as-cast) condition in comparison with the actual chemical composition of the alloy.

Element, at%	Al	Nb	Ti	V	Zr
Matrix	21.1	22.8	24.8	23.0	8.3
Second phase particles	27.4	13.2	11.2	21.1	27.1
Alloy composition	23.4	21.0	22.7	21.7	11.2

melting of the elements in a low-pressure, high-purity argon atmosphere inside a water-cooled copper cavity. The purities of the alloying elements were no less than 99.9 at%. The size of the produced ingot was $\sim 6\times 12\times 40~\text{mm}^3$. The chemical composition of the alloy measured by energy dispersive spectroscopy (EDS) closely corresponded to the nominal chemical composition (Table 1).

For the HPT processing discs with the diameter of 10 mm and thickness of 0.8 mm were cut from the cast AlNbTiVZr $_{0.5}$ alloy ingot, then ground and mechanically polished. The discs were subjected to HPT at room temperature to 0.25, 0.5, 1, and 5 revolutions of the anvil under a pressure of 8 GPa in a Bridgman anvil-type unit with the rate of 0.5 rpm using a custom-built computer-controlled HPT device (W. Klement GmbH, Lang, Austria).

Microstructure of the AlNbTiVZr $_{0.5}$ alloy in the initial (as-cast) condition and after HPT was studied using X-ray diffraction analysis (XRD), scanning (SEM) and transmission (TEM) electron microscopy. The XRD analysis was performed using a RIGAKU diffractometer with CuK α radiation. A PowderCell software (v. 2.4) was used for the qualitative phase analysis. The obtained XRD data was also used for the calculation of a long-range order parameter (LROP) by comparing intensities of the fundamental and superlattice reflections. A detailed description of the procedure can be found elsewhere [36].

The samples for SEM observations were prepared by careful mechanical polishing. SEM back-scattered electron (BSE) images of microstructures were obtained using FEI Quanta 3D microscope equipped with an EDS detector. The actual chemical composition of the alloy was measured by EDS scanning over the area $\approx 0.5 \times 0.5 \ \text{mm}^2$. SEM examinations were carried out in a mid-thickness of a transversal section in three different characteristic areas: (i) in the central part of the disc, i.e. within \pm 0.5 mm from the center; (ii) at the half of the radius, i.e. \sim 2.5 mm from the center; (iii) at the edge, i.e. \sim 4–5 mm from the center. Dimensions and the volume fraction of phases were measured by a Digimizer Image Analysis Software using SEM-BSE images.

TEM examinations were performed in a mid-thickness of the specimens in the shear plane in the vicinity ($\sim 1.5~\text{mm}$ away) of the edge. Samples for the TEM analysis were prepared by a conventional twin-jet electropolishing at a temperature of - 35 °C and an applied voltage of

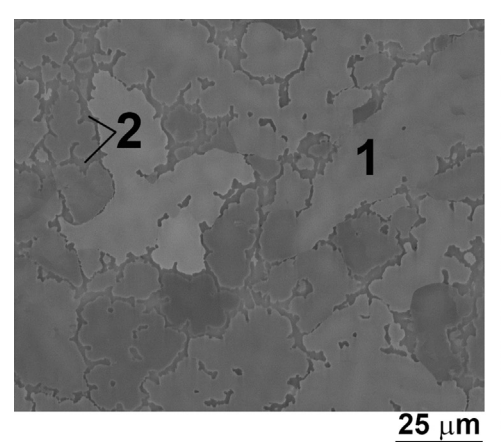
29.5~V in a mixture of 600~ml of methanol, 360~ml of butanol and 60~ml of perchloric acid. The TEM investigations were performed using a JEOL JEM-2100 microscope at an accelerating voltage of 200~kV.

Both microhardness measurements and nanoindentation tests were used to study mechanical properties evolution of the AlNbTiVZr_{0.5} alloy during HPT. The microhardness was measured in a transversal section in 5 different areas: in the central part of the disc and then per 1 mm away from the center. Each of the presented values represents the average of at least 10 measurements. Nanoindentation was performed in a transversal section of the specimens at the half of the radius using a Shimadzu DUH-211 s Dynamic Ultra Micro Hardness Tester with a 136degree Vickers diamond pyramid under a 50 mN load and a speed 6.6620 mN/s applied for 5 s. Both the Vickers nanohardness and Young's modulus of constitutive phases were determined during nanoindentation. Specific attention was paid to ensure that the indents were fully located inside the desired phases and did not overlap the other one. Only accurate indention results were taken for the further consideration. The size of the indents inside the B2 and Laves phases was 2.5-3.3 µm and 1.4-2.0 µm, respectively. Each of the presented values was the average of at least 5 measurements.

3. Results

Fig. 1 shows the structure of the AlNbTiVZr $_{0.5}$ alloy in the initial (ascast) condition. The structure was presented by coarse irregularly shaped matrix phase grains (labeled as 1 in Fig. 1a) and almost continuous chains of second phase particles (labeled as 2 in Fig. 1a) separating matrix grains. The average size of the matrix grains was \approx 25 μm , and the average size (thickness) of the second phase particles was \approx 2.5 μm . The volume fraction of the second phase particles was 19%. The results of the EDX analysis demonstrated that the particles were enriched with Al and Zr, and depleted of Nb and Ti (Table 1). The matrix phase had the composition close to the nominal concentrations. The results of the TEM analysis demonstrated that the matrix phase had a B2 ordered structure, while the second phase particles were a C14 (hexagonal) Laves phase (Fig. 1b).

The XRD pattern of the AlNbTiVZr $_{0.5}$ alloy in the initial (as-cast) condition (Fig. 2a) also demonstrated the presence of two phases: the B2 and C14 Laves phase. Much higher intensity of the B2 diffraction maximums was in agreement with the B2 structure of the matrix phase according to the TEM results (Fig. 1b). The XRD analysis had not revealed any noticeable changes in the phase composition of the AlNbTiVZr $_{0.5}$ alloy during HPT (Fig. 2a). The qualitative analysis demonstrated that the fractions of the B2 and Laves phases were $86.0 \pm 0.3\%$ and $14.0 \pm 0.2\%$, respectively, in all conditions. However, the Bragg peaks belonging to both phases broadened with an increase in the revolutions numbers, most possibly due to both defects generation and



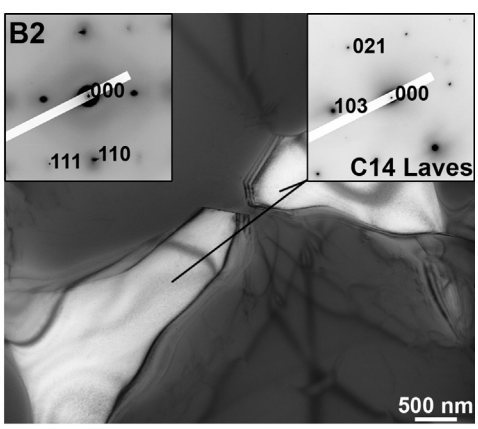


Fig. 1. Microstructure of the AlNbTiVZr $_{0.5}$ alloy in the initial (as-cast) condition, a – SEM-BSE image, b – TEM image.

b

Download English Version:

https://daneshyari.com/en/article/7973518

Download Persian Version:

https://daneshyari.com/article/7973518

<u>Daneshyari.com</u>